Applied Surface Science 257 (2011) 7204–7209

Contents lists available at ScienceDirect

Applied Surface Science

journal homepage: www.elsevier.com/locate/apsusc

Mechanical and optoelectric properties of post-annealed fluorine-doped tin oxide films by ultraviolet laser irradiation

Shih-Feng Tseng[a,b,*], Wen-Tse Hsiao[a], Donyau Chiang[a], Kuo-Cheng Huang[a], Chang-Pin Chou[b]

[a] Instrument Technology Research Center, National Applied Research Laboratories, Hsinchu 30076, Taiwan
[b] Department of Mechanical Engineering, National Chiao Tung University, Hsinchu 30010, Taiwan

ARTICLE INFO

Article history:
Received 29 November 2010
Received in revised form 15 March 2011
Accepted 15 March 2011
Available online 22 March 2011

Keywords:
Fluorine-doped tin oxide (FTO)
UV laser irradiation
Post-annealing
Mechanical property
Optoelectric property

ABSTRACT

The fluorine-doped tin oxide (FTO) thin film deposited on a soda–lime glass substrate was annealed by a defocus ultraviolet (UV) laser irradiation at ambient temperature. The mechanical and optoelectric properties of FTO films annealed by using the various laser processing parameters were reported. After the FTO films were subjected to laser post-annealing, the microhardness were slightly less but the reduced modulus values were larger than that of unannealed FTO films, respectively. The average optical transmittance in the visible waveband slightly increased with increasing the laser annealing energy and scan speed. Moreover, all the sheet resistance of laser annealed films was less than that of the unannealed ones. We found that the sheet resistance decrease was obviously influenced by annealing. The suitable annealing conditions could maintain the film thickness and relief the internal stress generated in the film preparation process to improve the electrical conductivity via decreasing laser energy or increasing scan speed.

1. Introduction

Recently, the developed fluorine-doped tin oxide (FTO) thin films were attracted much attention to meet the requirements of high transparency and low sheet resistance. Because the FTO thin films contain no expensive indium (In) element, this transparent conductive material cost is in general less than other transparent conductive oxides (TCOs) containing In. The FTO thin films are gradually accepted to apply as the conductive material for the flat panel displays, touch panels, flexible electronics, dye-sensitized solar cells (DSSC), light-emitting diodes (LEDs), and other optoelectronics products [1–7]. On the other hand, the traditional annealing process involves treating whole workpieces in heat treatment furnaces. This annealing equipment is unsuitable for manufacturing products which consisted of the low melting temperature materials because these materials are easily deformed or melt under the long annealing time intervals. Therefore, a novel laser processing technique was developed to anneal a thin film layer deposited on the various material substrates including different melting materials due to its short pulse duration, high pulse repetition frequency, and high laser power.The thin films annealed using different laser sources and processing skills were discussed. Chung et al. [8] adopted a XeCl excimer laser (λ: 308 nm) to anneal indium tin oxide (ITO) films deposited at 25 °C on 100 mm Corning 1737 glass substrates by DC magnetron sputtering. After laser annealing process optical and electrical characteristics of ITO films were significantly improved. The sheet resistance of annealed films decreased from 191 Ω/□ to 25 Ω/□, and the optical transmittance in the visible range increased from 70% to more than 85%, simultaneously. Kim et al. [9] used post-laser annealing to reduce the concentration of defects and to enlarge the gain sizes in the ZnO layer. A pulsed KrF excimer laser (λ: 248 nm) was applied by them to improve TFT characteristics. The ZnO-TFT first annealed in a furnace at 400 °C and then annealed by 200 laser pulses revealed the best TFT performance. The high mobility of 5.08 $cm^2/V s$ and low threshold voltage of 0.6 V were obtained in their evaluation results. Legeay et al. [10] investigated interactions between UV lasers and ITO films sputtered at room temperature. The annealed amorphous ITO films produced nanometric cracks and increased optical transmittance by a 308 nm excimer laser with laser exposures at fluences around 100 mJ/cm^2. Cheng et al. [11] utilized a femtosecond laser with an 80 MHz repetition rate to pattern crystalline ITO (c-ITO) patterns on amorphous ITO (a-ITO) thin films. The experimental results revealed that the a-ITO film was transformed into a c-ITO film via the heat accumulation energy supplied by the high repetition rate laser beam. Chen et al. [12] developed a Nd:YAG laser annealing process and combined the beam shaping technology with a top-hat intensity distribution to enhance the electrical properties of SnO_2:F (FTO) films. After the laser annealing pro-

* Corresponding author at: Instrument Technology Research Center, National Applied Research Laboratories, System Control and Integration Division, 20 R&D Road VI, Hsinchu Science Park, Hsinchu 30076, Taiwan. Tel.: +886 3 5779911x227; fax: +886 3 5773947.
E-mail address: tsengsf@itrc.narl.org.tw (S.-F. Tseng).

0169-4332/$ – see front matter. Crown Copyright © 2011 Published by Elsevier B.V. All rights reserved.
doi:10.1016/j.apsusc.2011.03.091

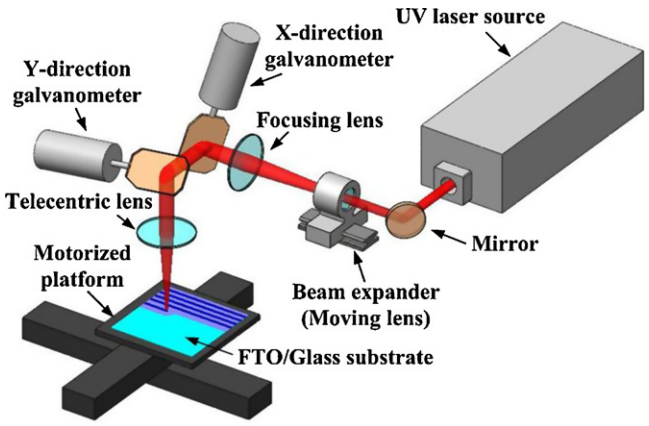

Fig. 1. Schematic diagram of UV laser annealing system.

cess, the sheet resistance was reduced from $639.7 \pm 40.02\ \Omega/\square$ to $595.1 \pm 29.0\ \Omega/\square$ while the carrier mobility was increased from $11.18 \pm 0.29\ cm^2/V\,s$ to $11.71 \pm 0.34\ cm^2/V\,s$. Ahn et al. [13] used a XeCl excimer laser annealing with a mask for reducing the contact resistance between amorphous-InGaZnO (a-IGZO) channel and source/drain layer in TFTs. After laser annealing with a laser energy density of 130 mJ/cm^2, the electrical resistivity of annealed a-IGZO TFTs was reduced from 10^4 to $3.2 \times 10^{-3}\ \Omega\,cm$. Moreover, these annealed TFTs exhibited better characteristics including a field-effect mobility of $21.79\ cm^2/V\,s$, a threshold voltage of -0.15 V, a sub-threshold swing of 0.26 V/decade, and an on/off ratio of 1.2×10^8. Chae et al. [14] proposed a high-resolution, large-area, and resistless patterning of ITO thin films using an excimer laser projection annealing process. A 60 nm thick a-ITO film deposited on a Corning 1737 glass substrate by sputtering was transformed into polycrystalline ITO (p-ITO) film after laser projection, and then the sharp and clean p-ITO patterns were obtained after wet etch process. Moreover, the patterned quality was suitable for high-volume production of flat-panel displays. Tseng et al. [15] discussed the characteristics of Ni–Ir and Pt–Ir hard coatings surface treated by a pulsed Nd:YAG laser (λ: 1064 nm). The laser treated films revealed high roughness, low microhardness and low reduced modulus because of the film oxidation occurred in high working temperature environment. Therefore, these films were unable to withstand the 1500 °C working temperature in the air, which temperature was considered for quartz molding process and hot embossing process.

This study focused on FTO thin film annealing and used an ultraviolet (UV) laser processing system combined with a direct writing technique. The processing parameters including the laser pulse energy, the pulse repetition rate, and the scanning speed of galvanometers were used to tune the annealed temperatures on the FTO film surface. After laser annealing, the microhardness and reduced modulus of the annealed films were evaluated by a nanoindentation instrument. In addition, the transmittance spectra and sheet resistivity of the annealed films were analyzed by a spectrophotometer and a four point probe instrument, respectively.

2. Experimental

2.1. UV laser annealing system

Fig. 1 shows the schematic diagram of the UV laser annealing system. A diode pumped Nd:YVO_4 UV laser processing system (Coherent, Inc. model AVIA 355-14) with the wavelength of 355 nm was used for post-annealing FTO films on glass substrates. The laser beam was delivered through a reflective mirror, a beam expander with 2× magnification, and a galvanometer system (Raylase AG model SS-15) with a focus shifter that could adjust the focus ranges in Z-direction from +15 mm to −15 mm. The telecentric lens was used in this system with the focal length of 110 mm and the scanning area of 40 mm × 40 mm that the designed incident laser beam was perpendicular to the film surface.

Table 1
UV laser system specification.

Wavelength (nm)	355
Maximal power (W) @ 100 kHz	14
Spatial mode	TEM_{00} ($M^2 < 1.3$)
Beam diameter, ±10% (mm)	3.5
Pulse repetition frequency (kHz)	1–300
Pulse width (ns) @ 100 kHz	28

In this laser operation system, several important specifications of UV laser were included below; the maximal power was 14 W, the transverse mode was TEM_{00}, and the maximal pulse repetition rate was 300 kHz. Each pulsed energy and pulsed width was of 170 μJ and 28 ns at the 100 kHz pulsed repetition rate. The nominal values of the laser beam diameter at the exit port and average spot size were approximately 3.5 mm and 15 μm, respectively. The completed specification of the UV laser processing system is presented in Table 1. The average output power, the pulse repetition rate, and the scanning speed of galvanometers on the FTO film surface were adjusted by a commercial software, which allows an automatic control operation during the laser annealing process.

2.2. Sample preparation

The FTO thin films were deposited on the soda–lime glass substrates by the sputtering method. An oxide buffer layer of SiO_2 composition was deposited on glass substrate surface to enhance adhesion between the FTO film and substrate. The thickness of FTO film and buffer layer was approximately 110 nm and 90 nm, respectively, measured by the SEM. Moreover, the thickness of the glass substrates was 1.1 mm. The deposited films were first annealed in a furnace at 400 °C. Fig. 2 shows a SEM cross-section view picture of FTO film deposited on the glass substrate. Table 2 summarizes the properties of FTO films deposited on a glass substrate used in this experiment. The average optical transmittance of FTO/glass substrate under the visible waveband region from 400 nm to 700 nm was measured to be 80.2%. Furthermore, the FTO film before laser annealing demonstrated sheet resistance, microhardness, and reduced modulus of 1030 Ω/□, 4.53 GPa, and 50.28 GPa, respectively. Fig. 3 shows the surface roughness in 3D

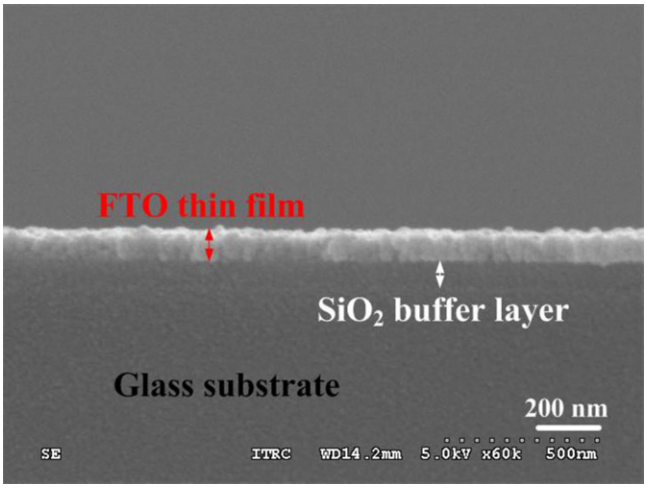

Fig. 2. A SEM cross-section view to illustrate the FTO thin film/SiO_2 buffer layer/glass substrate structure.

Table 2
Measured parameters of the FTO thin film deposited on glass substrates annealed in a furnace at 400 °C.

Measured parameters	FTO/glass
Thickness (film/substrate)	110 nm/1.1 mm
Transmittance (%) (400–700 nm)	80.2
Sheet resistance (Ω/□)	1030
Microhardness (GPa)	4.53
Reduced modulus (GPa)	50.28
Surface roughness (RMS, nm)	5.3

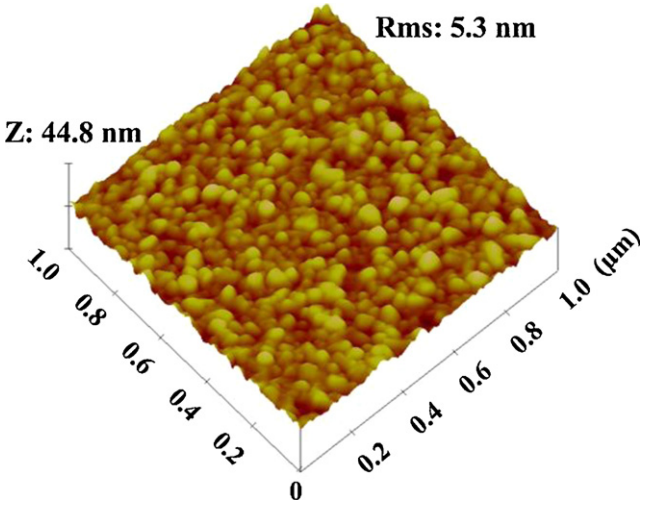

Fig. 3. Surface roughness of the FTO thin film annealed in a furnace at 400 °C.

images of the FTO thin film scanned by an atomic force microscope (Veeco di Dimension 3100, USA). The measured surface region was 1 μm × 1 μm. The measured root mean square (RMS) value of the FTO thin film was of 5.3 nm.

A spectrometer (Lambda 900 UV/Vis/NIR) was used to measure the transmittance and reflectance of the FTO/glass substrate. The measured data were shown in Fig. 4. The transmittance and reflectance values at 355 nm wavelength were approximately 71% and 24.6%, respectively. Therefore, the absorptance value at 355 nm

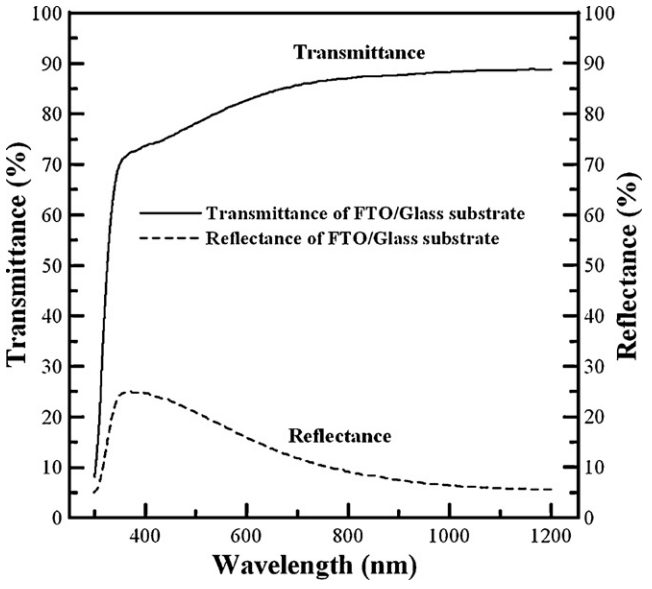

Fig. 4. Optical transmittance and reflectance versus wavelength for the FTO/glass substrate.

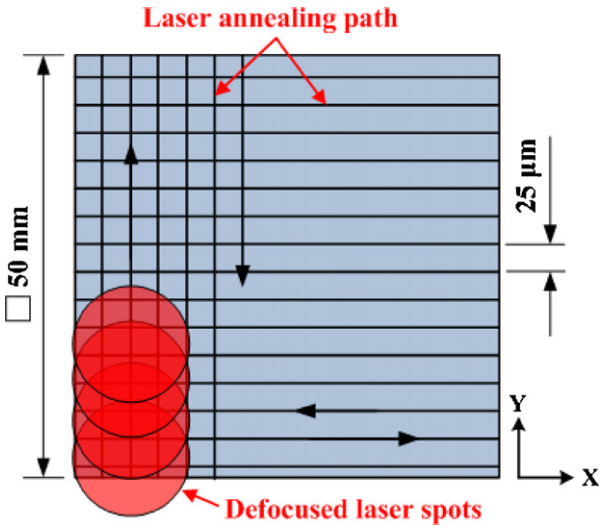

Fig. 5. Schematic diagram of the laser annealing paths.

wavelength was approximately 4.4% for the combined FTO/glass substrate workpiece.

2.3. UV laser annealing parameters

A nanosecond pulsed UV laser of 355 nm wavelength was used to anneal the electrode layer on the FTO/glass substrates. Fig. 5 shows schematically the laser annealing paths which were the cross lines in each X and Y direction with equal line-scan spacing. The dimensions of scan area and line-scan spacing were 50 mm × 50 mm and 25 μm, respectively. The experimental variables including laser pulsed energies of 165 μJ, 128 μJ, and 93 μJ and the scanning speeds of 200 mm/s, 400 mm/s, 600 mm/s, 800 mm/s, and 1000 mm/s were selectively adjusted to tune the annealed temperature on the FTO film surface. Moreover, the rest of experimental constrains were involved the pulse repetition rate of 100 kHz and the defocused spot size of 2 mm.

3. Results and discussion

3.1. Mechanical properties

After the FTO films were subjected to laser annealing with differing laser energy (E) and scan speed (V), tested results of microhardness and reduced modulus were measured by the nanoindentation instrument as shown in Figs. 6 and 7, respectively. The nanoindentation parameters consisting of loading, holding, and unloading times of 5 s for each step, indentation depth of 11 nm ± 10%, and the maximal loading of 200 μN were adopted in this study. Moreover, the average values from five tested points on each specimen with the corresponding standard deviation were introduced. The measured results reveal that the microhardness values of annealed FTO films are from 3.55 GPa to 4.42 GPa, and the averaged value from these tests is approximately located in 4 GPa, as shown in Fig. 6. All microhardness values of laser annealed FTO films are slightly less than that of unannealed FTO films due to the oxidation reaction between laser heating spot and oxide films [15,16]. Moreover, the microhardness error bar is larger than 1 GPa caused by rough FTO film surface. The similar large data fluctuations are observed in documents [15,17], and the fluctuations are contributed from the rough surface measurements. In addition, the measured results show that the values of reduced modulus for laser annealed FTO films are from 50.59 GPa to 58.13 GPa, and the averaged value from these tests is approximately concentrated in

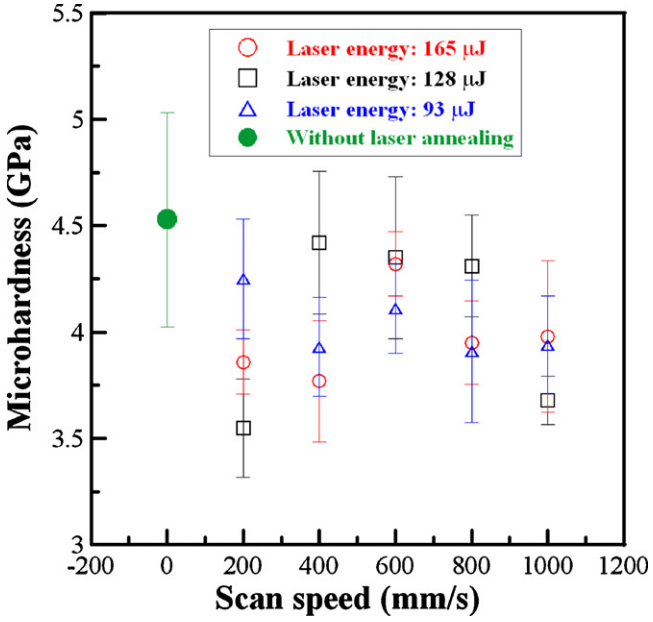

Fig. 6. Plot of microhardness results under different laser energy and scan speed.

54 GPa, as shown in Fig. 7. The reduced modulus values of laser annealed FTO films are larger than that of unannealed ones. The reduced module of FTO films calculated after laser annealing is higher than that of unannealed FTO films because of the stress relaxation.

3.2. Optical properties

The effect of annealing temperatures on the FTO films could be tuned by adjusting different laser energy and scanned speed [18–20]. Fig. 8 shows the transmittance spectra of FTO films for different annealing parameters, and Table 3 shows the average optical transmittance in the visible waveband (λ: 400–700 nm) and absorptance in the 355 nm wavelength. In the visible waveband, the FTO films with thickness of 110 nm deposited on a glass substrate after annealing in a furnace at 400 °C exhibit an average optical transmittance of 80.2%. Then the transmittance increases up to 84.1% after the film is laser annealed with E of 165 μJ and V of 1000 mm/s. The measured results reveal that the optical transmittance slightly increases with increasing the E and V values. Furthermore, the absorptance values of laser annealed FTO films are from 3.3% to 3.7% and are slightly lower than that of unannealed ones of 4.4%. The annealing on the FTO films resulted in oppositely lower extinction coefficient [21]. Therefore, the laser annealing temperature has the strong effects to enhance the optical transmittance of FTO film for this study.

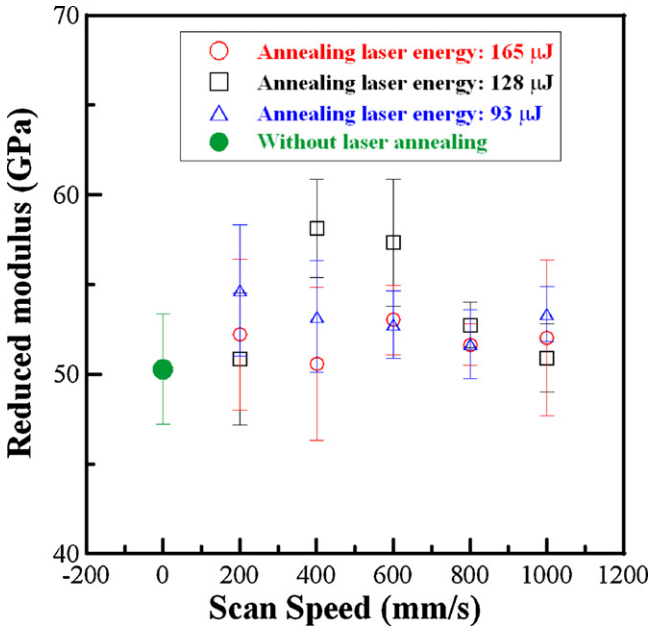

Fig. 7. Plot of reduced modulus results under different laser energy and scan speed.

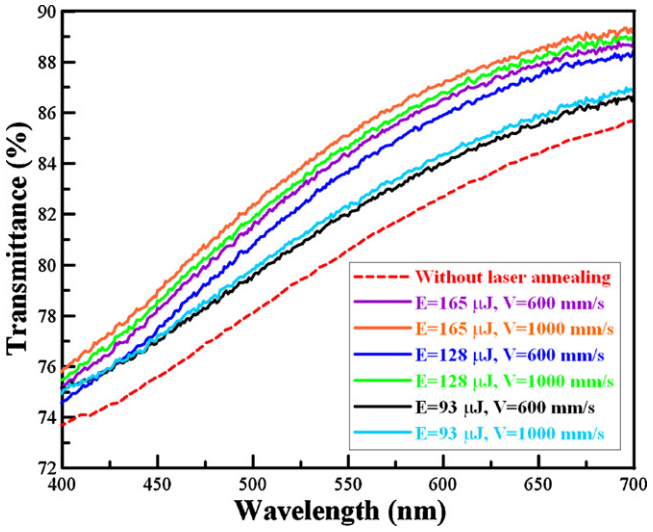

Fig. 8. Optical transmittance of visible wavelength for various annealed FTO films.

3.3. Electrical properties

The electrical property of the FTO films could be influenced by the annealing temperatures through the different E and V value adjustments. Fig. 9 shows the variation of sheet resistance as functions of laser energy and scanned speed for the FTO films. All sheet resistance of laser annealed FTO films decreased significantly compared with the original sheet resistance of 1030 Ω/□. Due to the accumulated temperatures increase on films surface to relieve the internal stress, the grain size of annealed FTO films increased and the distance between two neighboring grain boundaries increased that resulted in the lower sheet resistance [22]. Fig. 10 shows surface topographic SEM images of FTO films (a) before and (b) after laser annealing to demonstrate the change of grain size. Before laser annealing, the FTO film surface shows the small and uniform grains, and the average size is calculated as 12.5 nm, shown in Fig. 10(a). The crystalline grains become larger when the FTO films were annealed using scan speed of 600 mm/s and laser energy of 165 μJ. Moreover, cubical-shaped grains with an average 35.7 nm

Table 3
Average optical transmittance of FTO film annealed at different laser parameters.

Laser annealing parameters	Average optical transmittance (%, λ: 400–700 nm)	Absorptance (%, λ: 355 nm)
E = 165 μJ, V = 600 mm/s	83.5	3.5
E = 165 μJ, V = 1000 mm/s	84.1	3.3
E = 128 μJ, V = 600 mm/s	82.8	3.6
E = 128 μJ, V = 1000 mm/s	83.7	3.4
E = 93 μJ, V = 600 mm/s	81.5	3.7
E = 93 μJ, V = 1000 mm/s	81.8	3.7

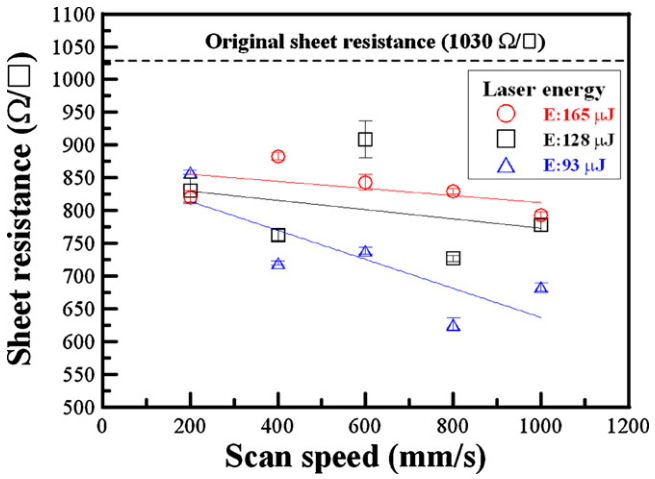

Fig. 9. Sheet resistance of FTO films after laser annealing with different processing parameters.

diameter are observed on the annealed film surface as shown in Fig. 10(b).

According to the resistance equation of $R = (\rho)/d$, the sheet resistance (R) of thin films was directly proportion to the resistivity (ρ) and was reversely proportion to the film thickness (d). The measured results showed that the sheet resistance of laser annealed FTO films obviously decreased by decreasing E values and increasing V values because the stress in the film was relaxed and the film thickness was unchanged due to less laser exposure energy density. The high laser power density annealing could have detrimental effect on the film structure and thickness through the violent laser interaction [23]. Hence, the lowest sheet resistance of 627 Ω/□ was obtained from the film that was annealed at laser energy of 93 μJ and scan speed of 800 mm/s. However, we used the defocused spot size of 2 mm to anneal these FTO thin films. The laser-annealing fluence is ranging from 3 mJ/cm^2 to 5.3 mJ/cm^2 that is much lower than the ablation threshold of the FTO film conducted by the UV laser to be 3.5 J/cm^2, three orders higher than our experimental variables, which cannot ablate FTO layers on glass substrate.

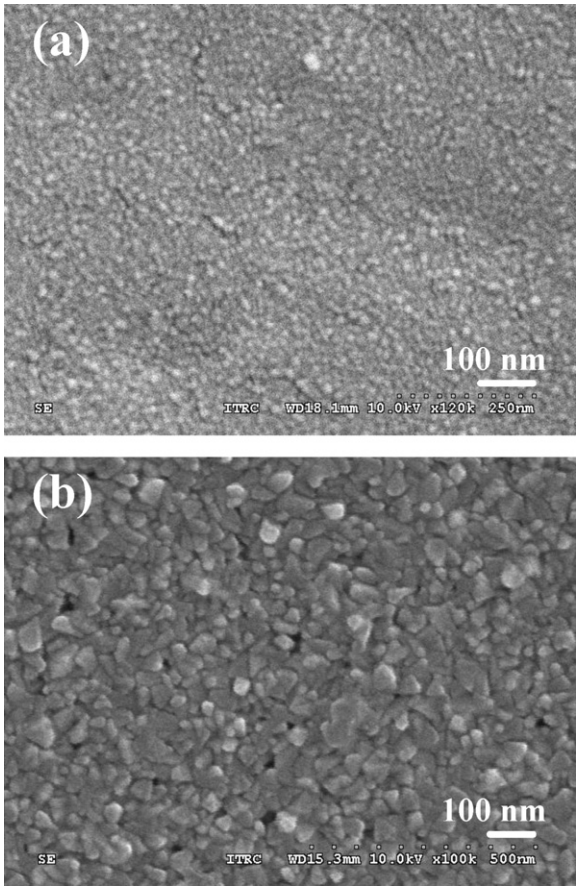

Fig. 10. SEM micrographs of FTO films (a) before and (b) after laser annealing with scan speed of 600 mm/s and laser energy of 165 μJ.

4. Conclusions

FTO films deposited on glass substrates were annealed using the direct writing technology by the nanosecond pulsed UV laser system. The microhardness of laser annealed FTO films was slightly less but the reduced modulus was larger than that of unannealed FTO films. The average optical transmittance of laser annealed FTO films in the visible waveband slightly increased with increasing the laser energy. Moreover, the value of average optical transmittance for laser annealed FTO films increased approximately 4% compared with unannealed FTO films. All the sheet resistance of laser annealed FTO films decreased significantly compared with the original sheet resistance. The proper working windows to relax the film stress without seriously damaging the film, we found were suitable to reduce the values of sheet resistance through increasing the scanned speed or decreasing the laser energy density.

Acknowledgements

The authors thank the National Science Council of Taiwan for financially supporting this research under contract no. NSC 99-2221-E-492-004 and no. NSC 98-2218-E-492-001, and the instrument supports from Instrument Technology Research Center, Taiwan are also acknowledged.

References

[1] B. Yoo, K.J. Kim, S.Y. Bang, M.J. Ko, K. Kim, N.G. Park, Chemically deposited blocking layers on FTO substrates: effect of precursor concentration on photovoltaic performance of dye-sensitized solar cells, J. Electroanal. Chem. 638 (2010) 161–166.
[2] Z. Tachan, S. Rühle, A. Zaban, Dye-sensitized solar tubes: a new solar cell design for efficient current collection and improved cell sealing, Sol. Energy Mater. Sol. Cells 94 (2010) 317–322.
[3] A.G. Macedo, E.A. de Vasconcelos, R. Valaski, F. Muchenski, E.F. da Silva Jr., A.F. da Silva, L.S. Roman, Enhanced lifetime in porous silicon light-emitting diodes with fluorine doped tin oxide electrodes, Thin Solid Films 517 (2008) 870–873.
[4] M.S. Akhtar, J.H. Hyung, T.H. Kim, O.B. Yang, S.K. Lee, ZnO nanorod-TiO_2-nanoparticulate electrode for dye-sensitized solar cells, Jpn. J. Appl. Phys. 48 (2009) 125003.
[5] C.J. Lin, W.Y. Yu, S.H. Chien, Transparent electrodes of ordered opened-end TiO_2-nanotube arrays for highly efficient dye-sensitized solar cells, J. Mater. Chem. 20 (2010) 1073.
[6] J. Chen, K. Li, Y. Luo, X. Guo, D. Li, M. Deng, S. Huang, Q. Meng, A flexible carbon counter electrode for dye-sensitized solar cells, Carbon 47 (2009) 2704.
[7] D. Li, C. Ding, H. Shen, Y. Liu, Y. Zhang, M. Li, J. Yan, Large improvement of photon capture for a dye-sensitized solar cell integrated with a fluorescent layer, J. Phys. D: Appl. Phys. 43 (2010) 015101.
[8] W. Chung, M.O. Thompson, P. Wickboldt, D. Toet, P.G. Carey, Room temperature indium tin oxide by XeCl excimer laser annealing for flexible display, Thin Solid Films 460 (2004) 291–294.
[9] J.J. Kim, J.Y. Bak, J.H. Lee, H.S. Kim, N.W. Jang, Y.Y. Yun, W.J. Lee, Characteristics of laser-annealed ZnO thin film transistors, Thin Solid Films 518 (2010) 3022–3025.
[10] G. Legeay, X. Castel, R. Benzerga, J. Pinel, Excimer laser beam/ITO interaction: from laser processing to surface reaction, Phys. Stat. Sol. 5 (2008) 3248–3254.
[11] C.W. Cheng, C.T. Lin, W.C. Shen, Y.J. Lee, J.S. Chen, Patterning crystalline indium tin oxide by high repetition rate femtosecond laser-induced crystallization, Thin Solid Films 518 (2010) 7138–7142.
[12] M.F. Chen, K.M. Lin, Y.S. Ho, Effects of laser-induced recovery process on conductive property of SnO_2:F thin film, Mater. Sci. Eng. B 176 (2011) 127–131.
[13] B.D. Ahn, W.H. Jeong, H.S. Shin, D.L. Kim, H.J. Kim, J.K. Jeong, S.H. Choi, M.K. Han, Effect of excimer laser annealing on the performance of amorphous indium gal-

lium zinc oxide thin-film transistors, Electrochem. Solid-State Lett. 12 (2009) H430.
[14] J. Chae, L. Jang, K. Jain, High-resolution, resistless patterning of indium-tin-oxide thin films using excimer laser projection annealing process, Mater. Lett. 64 (2010) 948–950.
[15] S.F. Tseng, W.T. Hsiao, K.C. Huang, M.F. Chen, C.T. Lee, C.P. Chou, Characteristics of Ni–Ir and Pt–Ir hard coatings surface treated by pulsed Nd:YAG laser, Surf. Coat. Technol. 205 (2010) 1979–1984.
[16] Y.C. Chim, X.Z. Ding, X.T. Zeng, S. Zhang, Oxidation resistance of TiN, CrN, TiAlN and CrAlN coatings deposited by lateral rotating cathode arc, Thin Solid Films 517 (2009) 4845–4849.
[17] M. Palacio, B. Bhushan, Nanomechanical characterization of adaptive optics components in microprojectors, J. Micromech. Microeng. 20 (2010) 064002.
[18] G. Gonçalves, E. Elangovan, P. Barquinha, L. Pereira, R. Martins, E. Fortunato, Influence of post-annealing temperature on the properties exhibited by ITO, IZO and GZO thin films, Thin Solid Films 515 (2007) 8562–8566.
[19] D. Wan, Y. Wang, B. Wang, C. Ma, H. Sun, L. Wei, Effects of the crystal structure on electrical and optical properties of pyrite FeS_2 films prepared by thermally sulfurizing iron films, J. Cryst. Growth 253 (2003) 230–238.
[20] H.J. Cho, S.U. Lee, B. Hong, Y.D. Shin, J.Y. Ju, H.D. Kim, M. Park, W.S. Choi, The effect of annealing on Al-doped ZnO films deposited by RF magnetron sputtering method for transparent electrodes, Thin Solid Films 518 (2010) 2941–2944.
[21] O. Lupan, T. Pauporté, L. Chow, B. Viana, F. Pellé, L.K. Ono, B. Roldan Cuenya, H. Heinrich, Effects of annealing on properties of ZnO thin films prepared by electrochemical deposition in chloride medium, Appl. Surf. Sci. 256 (2010) 1895–1907.
[22] S. Lee, J. Seong, D.Y. Kim, Effects of laser-annealing using a KrF excimer laser on the surface, structural, optical, and electrical properties of AlZnO thin films, J. Korean Phys. Soc. 56 (2010) 782–786.
[23] M.H. Badawi, B.J. Sealy, K.G. Stephens, Vaporisation of GaAs during laser annealing, Electron. Lett. 15 (1979) 786–787.